BOUNDARY LAYER FLOW OF SISKO FLUID WITH CONVECTIVE BOUNDARY CONDITIONS

SABIKA MALIK

Master of Science
in
Computational Science and Engineering

Research Centre for Modeling and Simulation
National University of Sciences and Technology
January, 2015
Islamabad, Pakistan

BOUNDARY LAYER FLOW OF SISKO FLUID WITH CONVECTIVE BOUNDARY CONDITIONS

SABIKA MALIK
(2011-NUST-MS PhD-CS&E-21)

A thesis submitted to Research Centre for Modeling and Simulation National University of Sciences and Technology in partial fulfillment of the requirements for the degree of

Master of Science
in
Computational Science and Engineering

Dr. Meraj Mustafa Hashmi

Dr. Khalid Parvez

Dr. Adnan Maqsood

Mr. Ammar Mushtaq

BOUNDARY LAYER FLOW OF SISKO FLUID WITH CONVECTIVE BOUNDARY CONDITIONS

ABSTRACT

The study of boundary layer flows of non-Newtonian fluids has attracted much attention in the past because of its relevance in various industrial and engineering processes. Due to complexity of such fluids, several non-Newtonian fluid models have been proposed. With the growing importance of non-Newtonian fluids in modern technology and industries, the investigations of such fluids are desirable. A number of industrially important fluids including molten plastics, pulps, polymers, polymeric melts, foods and fossil fuels, which may saturate in underground beds, display non-Newtonian behaviors. These include shear thinning, shear thickening, viscoelasticity, yield stress etc. Sisko fluid model is one of the non-Newtonian fluid models that can be utilized to predict the shear-thinning as well as shear-thickening fluids. In spite of its wide occurrence in industry, only limited studies have been reported on the flow of Sisko fluids.

In this work a mathematical model is developed to investigate the flow of Sisko fluid in the presence of convective boundary conditions. The governing nonlinear partial differential equations are reduced to a system of nonlinear ordinary differential equations via similarity transformations. An analytical approach namely homotopy analysis method (HAM) is used to compute analytic solutions. Unlike perturbation methods, the HAM is independent of small/large physical parameters, and thus is valid no matter whether a non-linear problem contains small/large physical parameters or not.

More importantly, different from all perturbation and traditional non-perturbation methods, the HAM provides us a simple way to ensure the convergence of solution series, and therefore, the HAM is valid even for strongly nonlinear problems.

DEDICATION

To my family for their prayers and support, that enabled me to carry out my studies.

ACKNOWLEDGEMENTS

In the Name of ALLAH, The Most Beneficent and The Most Merciful. First of all thanks to Almighty Allah (Who is the creator of all human being), Who have given me the strength and knowledge to complete this project.

I would like to thank to my parents and whole family members for there help, support and prayers. It is because of their love and encouragement that I have been able to complete this project.

I wish to acknowledge the continuous help and valuable instructions from my sincere and most cooperative supervisor Dr. Meraj Mustafa Hashmi. His positive outlook and confidence in my research inspired me gave me confidence.

I am extremely thankful to Dr. Adnan Maqsood for his enormous help and valuable suggestions during my research.

I would like to thank to Mr. Ammar Mushtaq for his constant help during my research.

CONTENTS

List of Figures

List of Tables

INTRODUCTION

1.1 Basic Definitions and Involved Concepts

1.1.1 Newtonian and non-Newtonian Fluids

Many fluids we encounter in industrial applications deviate from the classical Newton's law of viscosity which states that the shear stress is directly and linearly proportional to the rate of deformation. The fluids which obey this law are termed as Newtonian fluids. Examples include water, milk, sulphuric acid, carosine, air and thin motor oil etc. The fluids which exhibit a nonlinear relationship between the shear stress and the deformation rate are non-Newtonian fluids. Examples include multigrade oils gypsum pastes, polymers, printer inks, blood, fruit juices etc.

1.1.2 Classification of Non-Newtonian Fluids

Non-Newtonian fluids are categorized as below:

i. Time-independent Fluids

- **Bingham Plastic**

The fluids which behave like a rigid body at low stresses but flows as a viscous fluid at high stress are called bingham plastic. For example; toothpaste, mayonnaise.

- **Pseudo-plastic (Shear-thinning)**

The fluids in which viscosity decreases as the shear rate increases are known as shear-thinning fluids. Ketchup, blood, whipped cream, paints and many polymers are the examples of pseudo-plastic fluids.

- **Dilatant (Shear-thickening)**

The fluids in which viscosity increases as the shear rate increases are known as shear thickening fluids. Examples include beach sand, starch in water etc.

ii. Time-dependent Fluids

- **Thixotropic**

The fluids in which viscosity decreases with time for which stress is applied are known as thixotropic fluids. Their examples include drilling mud, certain gels and thixotropic jelly paints.

- **Rheopectic**

The fluids in which viscosity increases with time for which stress is applied are known as rheopectic fluids. For example; gypsum paints and printer inks.

iii. Viscoelastic Fluids

The fluids which return back to their original shape when the stress is released are known as viscoelastic fluids.

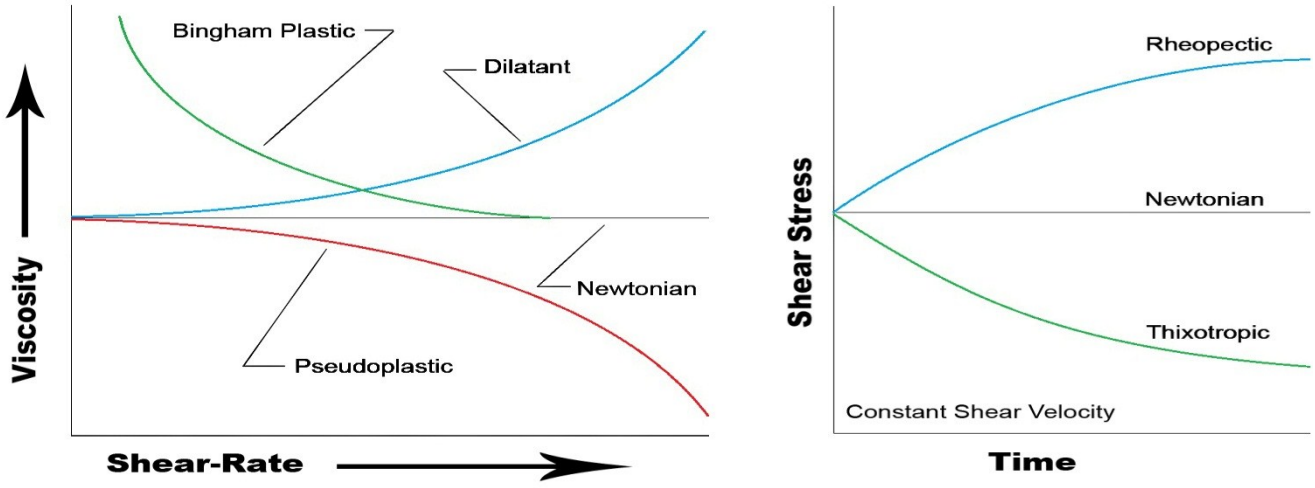

(a) **(b)**

Figure 1.1: Non-Newtonian Fluids

1.2 Constitutive Equations for Sisko Fluid

The constitutive equations for Sisko fluid are expressed as:

$$\rho \frac{d\boldsymbol{V}}{dt} = div\, \boldsymbol{\tau}, \tag{1.1}$$

where $\boldsymbol{V}$ is the velocity vector, ρ the density of the fluid and $\boldsymbol{\tau}$ is the Cauchy stress tensor for Sisko fluid given by:

$$\boldsymbol{\tau} = -pI + \boldsymbol{S}\ ; \qquad \boldsymbol{S} = \left[a + b\left|\sqrt{\frac{1}{2} tr \boldsymbol{A}_1^2}\right|^{n-1}\right]\boldsymbol{A_1}\ , \tag{1.2}$$

where p is the pressure, $\boldsymbol{S}$ is the extra stress tensor a, b and n are the material fluid parameters and $\boldsymbol{A_1} = (\boldsymbol{\nabla V}) + (\boldsymbol{\nabla V})^T$ is the first Rivlin-Ericksen tensor [1].

For a two-dimensional flow, we assume the velocity and the stress fields of the following forms.

$$\boldsymbol{V} = [u\,(x,y)\,, v\,(x,y)\,, 0]\,, \qquad \boldsymbol{S} = \boldsymbol{S}\,(x,y), \tag{1.3}$$

After using equations (1.2) and (1.3) in (1.1) we obtain:

$$\rho\left(u\frac{\partial u}{\partial x}+v\frac{\partial u}{\partial y}\right)=-\frac{\partial p}{\partial x}+a\left(\frac{\partial^2 u}{\partial x^2}+\frac{\partial^2 u}{\partial y^2}\right)+2b\frac{\partial}{\partial x}\left[\frac{\partial u}{\partial x}\left|4\left(\frac{\partial u}{\partial x}\right)^2+\left(\frac{\partial u}{\partial y}+\frac{\partial v}{\partial x}\right)^2\right|^{\frac{n-1}{2}}\right]+b\frac{\partial}{\partial y}\left[\left(\frac{\partial u}{\partial y}+\frac{\partial v}{\partial x}\right)\left|4\left(\frac{\partial u}{\partial x}\right)^2+\left(\frac{\partial u}{\partial y}+\frac{\partial v}{\partial x}\right)^2\right|^{\frac{n-1}{2}}\right], \tag{1.4}$$

$$\rho\left(u\frac{\partial v}{\partial x}+v\frac{\partial v}{\partial y}\right)=-\frac{\partial p}{\partial y}+a\left(\frac{\partial^2 v}{\partial x^2}+\frac{\partial^2 v}{\partial y^2}\right)+b\frac{\partial}{\partial x}\left[\left(\frac{\partial u}{\partial y}+\frac{\partial v}{\partial x}\right)\left|4\left(\frac{\partial u}{\partial x}\right)^2+\left(\frac{\partial u}{\partial y}+\frac{\partial v}{\partial x}\right)^2\right|^{\frac{n-1}{2}}\right]+2b\frac{\partial}{\partial y}\left[\frac{\partial v}{\partial y}\left|4\left(\frac{\partial u}{\partial x}\right)^2+\left(\frac{\partial u}{\partial y}+\frac{\partial v}{\partial x}\right)^2\right|^{\frac{n-1}{2}}\right], \tag{1.5}$$

The problem corresponds to the case of power-law fluid when $a=0$. The Eqs. (1.4) and (1.5) reduce to the Newtonian fluid case by choosing $b=0$. To non-dimensionalize equations (1.4) and (1.5), we introduce the following dimensionless variables:

$$u^*=\frac{u}{U},v^*=\frac{v}{U},x^*=\frac{x}{L},y^*=\frac{y}{L},p^*=\frac{p}{\rho U^2}, \tag{1.6}$$

where L and U are the characteristic length and the stretching velocity respectively.

In view of Eq. (1.6), Eqs (1.4) and (1.5) take the following forms:

$$\frac{\partial u^*}{\partial x^*}+\frac{\partial v^*}{\partial y^*}=0, \tag{1.7}$$

$$u^*\frac{\partial u^*}{\partial x^*}+v^*\frac{\partial u^*}{\partial y^*}=-\frac{\partial p^*}{\partial x^*}+\varepsilon_1\left(\frac{\partial^2 u^*}{\partial x^{*2}}+\frac{\partial^2 u^*}{\partial y^{*2}}\right)+2\varepsilon_2\frac{\partial}{\partial x^*}\left[\frac{\partial u^*}{\partial x^*}\left|4\left(\frac{\partial u^*}{\partial x^*}\right)^2+\left(\frac{\partial u^*}{\partial y^*}+\frac{\partial v^*}{\partial x^*}\right)^2\right|^{\frac{n-1}{2}}\right]+\varepsilon_2\frac{\partial}{\partial y^*}\left[\left(\frac{\partial u^*}{\partial y^*}+\frac{\partial v^*}{\partial x^*}\right)\left|4\left(\frac{\partial u^*}{\partial x^*}\right)^2+\left(\frac{\partial u^*}{\partial y^*}+\frac{\partial v^*}{\partial x^*}\right)^2\right|^{\frac{n-1}{2}}\right], \tag{1.8}$$

$$u^*\frac{\partial v^*}{\partial x^*}+v^*\frac{\partial v^*}{\partial y^*}=-\frac{\partial p^*}{\partial y^*}+\varepsilon_1\left(\frac{\partial^2 v^*}{\partial x^{*2}}+\frac{\partial^2 v}{\partial y^{*2}}\right)+\varepsilon_1\frac{\partial}{\partial x^*}\left[\left(\frac{\partial u^*}{\partial y^*}+\frac{\partial v^*}{\partial x^*}\right)\left|4\left(\frac{\partial u^*}{\partial x^*}\right)^2+\left(\frac{\partial u^*}{\partial y^*}+\frac{\partial v^*}{\partial x^*}\right)^2\right|^{\frac{n-1}{2}}\right]+2\varepsilon_2\frac{\partial}{\partial y^*}\left[\frac{\partial v^*}{\partial x^*}\left|4\left(\frac{\partial u^*}{\partial x^*}\right)^2+\left(\frac{\partial u^*}{\partial y^*}+\frac{\partial v^*}{\partial x^*}\right)^2\right|^{\frac{n-1}{2}}\right], \tag{1.9}$$

where the dimensionless parameters ε_1 and ε_2 are defined as

$$\varepsilon_1 = \frac{a/\rho}{LU} \text{ and } \varepsilon_2 = \frac{b/\rho}{LU}\left(\frac{U}{L}\right)^{n-1}, \tag{1.10}$$

Using the standard boundary layer assumptions $x^* \sim O(1)$, $u^* \sim O(1)$, $p^* \sim O(1)$, $v^* \sim O(\delta)$, $y^* O \sim (\delta)$, and the dimensionless coefficients $\varepsilon_1 \sim O(\delta^2)$ and $\varepsilon_2 \sim O(\delta^{n+1})$, Eqs (1.8) and (1.9) reduce to:

$$\frac{\partial u}{\partial x} + \frac{\partial v}{\partial y} = 0, \tag{1.11}$$

$$\rho\left(u\frac{\partial u}{\partial x} + v\frac{\partial u}{\partial y}\right) = -\frac{\partial p}{\partial x} + a\frac{\partial^2 u}{\partial y^2} + b\frac{\partial}{\partial y}\left(\left|\frac{\partial u}{\partial y}\right|^{n-1}\frac{\partial u}{\partial y}\right), \tag{1.12}$$

$$0 = -\frac{\partial p}{\partial y}, \tag{1.13}$$

1.3 Basic Idea of Homotopy Analysis Method (HAM)

Most of the problems in science and engineering are characterized by non-linear differential equations which are very difficult to solve analytically. Perturbation approach is an easy technique for solving non-linear problems analytically, but this method requires small or large parameter in the differential system. Such small/large parameter does not usually exist in physical problems. In contrast to non-perturbation methods such as artificial small parameter method [33], the δ-expansion method [34], the Adomian's decomposition method [35], and the homotopy perturbation method (HPM), HAM provides a simple procedure for adjusting and controlling the convergence region of the solutions.

In 1992 Liao [23] proposed such kind of analytic technique namely Homotopy analysis method (HAM). It is independent of small/large physical parameter and provides us with a convenient way to adjust the convergence region of nonlinear problems. In 2003 Liao discussed the basic ideas of HAM and its application in his book named "Beyond Perturbation" [26]. Thereafter the HAM attracts the attention of many researchers and has been applied to many nonlinear problems such as boundary layer flows, heat transfer, MHD

flows of non-Newtonian fluids and many others. Now a days HAM is successfully applied to many nonlinear flow problems [23-32].

For better understanding of the basic idea, let us consider the following differential equations:

$$\mathcal{N}[u(\xi)] = 0, \tag{1.14}$$

where $\boldsymbol{\mathcal{N}}$ is a non-linear operator, ξ denotes independent variable and $u(\xi)$ is an unknown function. Liao [26] constructed the so-called zero-order deformation equation in the following form.

$$(1-p)\mathcal{L}[\phi(\xi;p) - u_0(\xi)] = p\hbar H(\xi)\mathcal{N}[\phi(\xi;p)], \tag{1.15}$$

where $p\epsilon[0,1]$ is the embedding parameter, $\hbar \neq 0$ is a non-zero auxiliary parameter, $H(\xi) \neq 0$ is an auxiliary function, $\mathcal{L}$ is an auxiliary linear operator, $u_0(\xi)$ is an initial guess of $u(\xi)$ and $\phi(\xi;p)$ is a unknown function. When $p = 0$ Eq (1.15) gives the initial guess, final solution is retrieved by substituting $p = 1$.

$$\phi(\xi;0) = u_0(\xi)\,, \quad \phi(\xi;1) = u(\xi), \tag{1.16}$$

Expanding $\phi(\xi;p)$ in Taylor series $p = 0$, we have:

$$\phi(\xi;p) = u_0(\xi) + \sum_{m=1}^{\infty} u_m(\xi)p^m, \tag{1.17}$$

in which

$$u_m(\xi)\frac{1}{m!}\frac{\partial^m \phi(\xi;p)}{\partial p^m}\Big|_{p=0}, \tag{1.18}$$

If the auxiliary linear operator, the initial guess, the auxiliary parameter $\hbar$, and the auxiliary function are chosen properly, the series (1.17) converges at $p = 1$. In this case we have:

$$\phi(\xi;p) = u_0(\xi) + \sum_{m=1}^{\infty} u_m(\xi), \tag{1.19}$$

Differentiating Eq. (1.15) m times with respect to p and then setting $p = 0$ we obtain the so-called *m*th-order deformation equation as below:

$$\mathcal{L}[u_m(\xi) - \chi_m u_{m-1}(\xi)] = \hbar H(\xi) R_m(\vec{u}_{m-1}), \tag{1.20}$$

where

$$R_m(\vec{u}_{m-1}) = \frac{1}{(m-1)!} \frac{\partial^{m-1} \mathcal{N}[\phi(\xi;p)]}{\partial p^{m-1}}\bigg|_{p=0}, \tag{1.21}$$

and

$$\chi_m = \begin{cases} 0 & m \leq 1 \\ 1 & m > 1 \end{cases}.$$

1.4 Literature Review

The steady and unsteady flows over a stretching surface have wide range of applications such as production of plastic sheets, paper production, wire drawing, spinning of filaments and glass-fiber etc.

Figure 1.2: Stretching Sheet Applications

There is a significant difference in the solution of stretching flows and the laminar boundary layer flows induced by a stationary surface the so called Blasius flow [1].

Sakiadis [2] considered the momentum transport occurring in the boundary layer adjacent to a continuous surface moving steadily through a motionless fluid environment.

In contrast to Sakiadis [2], Crane [3] computed an exact similarity solution for the boundary layer flow of a Newtonian fluid towards an elastic sheet which is stretched with the velocity proportional to the distance from the origin.

Chen and Char [4] investigated the heat transfer occurring in the laminar boundary layer over a linearly stretching, continuous surface with suction or blowing. They considered two cases: (i) the sheet with prescribed wall temperature (ii) the sheet with prescribed heat flux. The solutions were obtained in the form of hyper geometric functions.

Cortell [5] presented numerical analysis for flow and heat transfer in a viscous fluid bounded by a nonlinearly stretching sheet. In this study, governing partial differential equations were first converted into ordinary differential equations by a similarity transformation. The arising equations were solved for the numerical solutions by standard shooting procedure. Later on, several studies concerning flow and heat transfer characteristics have been reported.

First of all, Schowalter [6] obtained the similar solutions for the boundary layer flow of power-law fluids. He obtained the two- and three-dimensional boundary-layer equations for pseudo-plastic non-Newtonian fluids. He determined the types of potential flows necessary for similar solutions of the boundary-layer equations.

Lee and Ames [7] studied the similarity solution for the non-Newtonian power law fluid. He obtained the numerical solution for forced convection of power law fluids about a right angled wedge.

Rajagopal and Gupta [8] studied the flow of an incompressible second-order fluid past a stretching sheet. They solved the boundary layer equations numerically using the Runge-Kutta method

Vajravelu and Rollins [9] studied the heat transfer characteristics in a viscoelastic fluid over a stretching sheet with frictional heating and internal heat generation or absorption. They considered two cases; (i) the sheet with prescribed surface temperature (ii) the sheet with prescribed wall heat flux.

Andersson and Bech [10] conducted a study on the magneto-hydrodynamic flow of an electrically conducting power-law fluid past a stretching sheet. The flow was subjected to a uniform transverse magnetic field. He found that the influence of magnetic field is to reduce boundary layer thickness.

Liao [12] analyzed the laminar boundary-layer flow and heat transfer of power-law non-Newtonian fluids over a stretching sheet by HAM.

All of the above mentioned studies are related to the boundary layer flows of Newtonian or non-Newtonian fluids over a stretching sheet. Amongst non-Newtonian fluid Sisko fluid model [13] is the one which can easily predict the shear thinning and thickening behavior of the fluid. It is a combination of power law and Newtonian fluid. Not much attention has been given till date to the flows of Sisko fluid.

Khan and Hayat [14] obtained an analytic solution for unidirectional flow of an electrically conducting Sisko fluid through a porous space. They solved the problem analytically using homotopy analysis method (HAM).

Hayat and Abelman [15] investigated the time-dependent flow of an incompressible Sisko fluid over a porous wall. The flow was caused by sudden motion of the wall in its own plane. The formulated nonlinear problem was solved by a symmetry approach.

Masood and Azeem [16] investigated the steady two-dimensional stagnation point flow of Sisko fluid over a stretching sheet. They transformed the governing boundary layer equation into non-linear ordinary differential equation and then obtained analytic solutions by HAM.

Convective boundary conditions are more general and practically useful especially metal drying process, thermal energy storage and many other engineering processes.

The pioneering work on heat transfer characteristics through convective boundary condition was presented by Aziz [17]. He studied the flow over a convectively heated stationary plate.

Yao etal [18] studied the heat transfer in a viscous fluid flow over a stretching/ shrinking sheet with a convective boundary condition. They obtained the solutions in the form of incomplete Gamma function. It is found the convective boundary conditions results in temperature slip at the wall and this temperature slip is largely influenced by the variation of embedded parameters.

Ishak [19] investigated the steady laminar boundary layer flow over a permeable flat plate in a uniform free stream. The bottom surface of the plate was heated by convection from a hot fluid. The arising differential system were computed numerically by shooting method.

Makinde and Aziz [20] investigated the boundary layer flow induced of a nanofluid by a convectively heated stretching sheet.

Makinde and Aziz [21] also investigated the heat and mass transfer from a vertical plate embedded in a porous medium considering the effects of a first-order chemical reaction and transverse magnetic field. The governing equations are solved numerically using a highly accurate and thoroughly tested finite difference algorithm.

Hayat and Shehzad [22] studied the flow and heat transfer in a second grade fluid over a stretching sheet subjected to convective boundary conditions. They utilized homotopy analysis method for obtaining convergent series solutions.

To the best of our knowledge the boundary layer flow of Sisko fluid over a stretching surface with convective boundary condition is not yet discussed. The main objective of this thesis is to develop the solution for this problem. The problem discussed in this thesis is nonlinear and is difficult to obtain its exact solution.

For this purpose a very powerful analytic technique namely Homotopy analysis method (HAM) is used to solve the nonlinear problem proposed by Liao [23, 24, 25]. HAM provides a appropriate way to control and adjust the convergence region and the rate of approximation and also, the HAM is independent of small or large parameter and is valid even if a nonlinear problem contains a small or large physical parameter or not.

ON STAGNATION POINT FLOW OF SISKO FLUID OVER A STRETCHING SHEET

This chapter contains the review on the recent work of The steady two-dimensional stagnation point flow of Sisko fluid over a stretching sheet is reviewed in this chapter. Similarity transformations are used to convert the boundary layer equations into similar forms. The solutions are obtained by using the homotopy analysis method (HAM). The HAM solutions are validated by the exact analytic solutions in a special case.

2.1 Problem Formulation

We consider the steady two-dimensional stagnation point flow of an incompressible Sisko fluid flowing towards a flat surface coinciding with the plane $y = 0$ and the flow being restricted to the region $y > 0$. The sheet is stretched in its own plane with the velocity $u_w = cx$. The boundary layer equations governing the steady two-dimensional stagnation point flow of Sisko fluid are as under:

$$\frac{\partial u}{\partial x} + \frac{\partial v}{\partial y} = 0, \tag{2.1}$$

$$u\frac{\partial u}{\partial x} + v\frac{\partial u}{\partial y} = U\frac{dU}{dx} + \frac{a}{\rho}\frac{\partial^2 u}{\partial y^2} + \frac{b}{\rho}\frac{\partial}{\partial y}\left(\left|\frac{\partial u}{\partial y}\right|^{n-1}\frac{\partial u}{\partial y}\right), \tag{2.2}$$

where u and v are the velocity components along the x and y directions respectively, a and b are the material fluid parameters, ρ is the fluid density n is the power law index $U(x) = dx$ is the free stream velocity.

When $a = 0$ the Eq (2.2) corresponds to the case of power law fluid and it reduces to the case of Newtonian fluid by substituting $b = 0$. In the present problem we have $\partial u/\partial y < 0$ when $d/c < 1$ and $\partial u/\partial y > 0$ when $d/c > 1$. Eq (2.2) can be expanded in these two cases as below.

$$u\frac{\partial u}{\partial x} + v\frac{\partial u}{\partial y} = U\frac{dU}{dx} + \frac{a}{\rho}\frac{\partial^2 u}{\partial y^2} - \frac{b}{\rho}\frac{\partial}{\partial y}\left(\frac{\partial u}{\partial y}\right)^n ; \quad d/c < 1 , \tag{2.3}$$

$$u\frac{\partial u}{\partial x} + v\frac{\partial u}{\partial y} = U\frac{dU}{dx} + \frac{a}{\rho}\frac{\partial^2 u}{\partial y^2} + \frac{b}{\rho}\frac{\partial}{\partial y}\left(\frac{\partial u}{\partial y}\right)^n ; \quad d/c > 1, \tag{2.4}$$

The boundary conditions for present problem are:

$$\begin{aligned} u = U_w(x) = cx, \; v = 0, \qquad & \text{at } y = 0, \\ u \to U(x) = dx, \qquad & \text{as} \qquad y \to \infty. \end{aligned} \tag{2.5}$$

Introducing the following similarity transformations:

$$\eta = y\left(\frac{c^{2-n}}{b/\rho}\right)^{\frac{1}{n+1}} x^{\frac{1-n}{1+n}}, \qquad \Psi(x,y) = \left(\frac{b/\rho}{c^{1-2n}}\right)^{\frac{1}{n+1}} x^{\frac{2n}{n+1}} f(\eta), \tag{2.6}$$

Eq (2.1) is identically satisfied and Eq (2.2) is reduced to the following form:

$$Af''' + n\left(f''(\eta) sgn\left(\frac{d}{c} - 1\right)\right)^{n-1} f''' + \left(\frac{2n}{n+1}\right) ff'' - f'^2 + \frac{d^2}{c^2} = 0, \tag{2.7}$$

The boundary conditions are:

$$f(0) = 0, \;\; f'(0) = 1, \;\; f'(\infty) = d/c, \tag{2.8}$$

where sgn(·) stands for sign function, A is the material fluid parameter of the Sisko fluid, Re_a and Re_b are the local Reynolds numbers. These parameters are defined as:

$$Re_a = \frac{\rho x U}{a}, \;\; Re_b = \frac{\rho x^n U^{2-n}}{b}, \;\; A = \frac{Re_b^{\frac{2}{n+1}}}{Re_a}, \tag{2.9}$$

The quantity of physical interest is the skin friction coefficient C_f which is defined as:

$$C_f = \tau_w / \left(\frac{1}{2}\rho U^2\right), \tag{2.10}$$

where $\tau_w = \left(a + b\left|\frac{\partial u}{\partial y}\right|^{n-1}\right)\frac{\partial u}{\partial y}\Big|_{y=0}$ is wall shear stress. Using variables from Eq (2.6), Eq (2.10) reduces to:

$$\frac{1}{2}C_f Re_b^{\frac{1}{n+1}} = Af''(0) — f''(0)sgn\left(\frac{d}{c} - 1\right)n, \tag{2.11}$$

2.2 Analytic Solution

2.2.1 The exact analytic solution

They only consider the case when n is a non-negative integer. For some special cases of the problem they first present the exact solution. When $d/c = 0$ and $n = 1$ Eq (2.7) with boundary condition (2.8), the exact solution is of the form:

$$f(\eta) = \sqrt{1+A}\left[1 - \exp\left(\frac{-\eta}{\sqrt{1+A}}\right)\right], \tag{2.12}$$

It should be noted here that if $A = 0$ the Eq. (2.12) reduces to the case of Newtonian fluid. When $d/c = 1$ Eq. (2.7) with boundary condition (2.8), has the exact solution.

$$f(\eta) = \eta, \tag{2.13}$$

2.2.2 Analytic solution for integer power-index when $d/c \neq 1$

We solve Eqs. (2.7) subject to the boundary conditions (2.8) with the help of HAM. The initial guess and linear operator selected as below.

$$f_0(\eta) = (d/c)\eta - \left[1 - exp\left(-\left|\frac{d}{c} - 1\right|\eta\right)\right]sgn\left(\frac{d}{c} - 1\right), \tag{2.14}$$

$$\mathcal{L}[\phi(\eta; p)] = \frac{\partial^3\phi(\eta;p)}{\partial\eta^3} - \frac{\partial^2\phi(\eta;p)}{\partial\eta^2}, \tag{2.15}$$

The operator $\mathcal{L}$ satisfies

$$\mathcal{L}[C_1 + C_2\eta + C_3\exp(-\eta)] = 0,$$

where $C_1, C_2\ and\ C_3$ are arbitrary constants.

2.2.2.1 Zero-order deformation problem

Now the problem related to zero order deformation is:

$$\hat{f}(\eta;p)=0,\ \ \widehat{f}'(\eta;p)=1,\quad \text{at}\,\eta=0,$$
$$\widehat{f}'(\eta;p)=d/c,\quad \text{as}\,\eta\to\infty. \tag{2.16}$$

$$(1-p)\mathcal{L}\left[\hat{f}(\eta;p)-f_0(\eta)\right]=p\hbar N_f\left[\hat{f}(\eta;p)\right], \tag{2.17}$$

where

$$N\left[\hat{f}(\eta;p)\right]=A\frac{\partial^3\hat{f}(\eta;p)}{\partial\eta^3}+n\left[\frac{\partial^2\hat{f}(\eta;p)}{\partial\eta^2}sgn\left(\frac{d}{c}-1\right)\right]^{n-1}\frac{\partial^3\hat{f}(\eta;p)}{\partial\eta^3}$$
$$+\left(\frac{2n}{n+1}\right)\hat{f}(\eta;p)\frac{\partial^2\hat{f}(\eta;p)}{\partial\eta^2}-\left[\frac{\partial\hat{f}(\eta;p)}{\partial\eta}\right]^2+\frac{d^2}{c^2}, \tag{2.18}$$

where $p\in[0,1]$ is an embedding parameter and $\hbar\neq 0$ is an auxiliary parameter. At $p=0$ and $p=1$ we have, respectively:

$$\hat{f}(\eta;0)=f_0(\eta),\ \hat{f}(\eta;1)=f(\eta). \tag{2.19}$$

When the parameter p varies from zero to unity the solution $\hat{f}(\eta;p)$ through the initial guess $f_0(\eta)$ approaches $f(\eta)$. Now we expand the function $\hat{f}(\eta;p)$ by using Taylor's series about $p=0$ and then substituting $p=1$, we get:

$$f(\eta)=f_0(\eta)+\sum_{m=1}^{\infty}f_m(\eta),\quad \text{where}\quad f_m(\eta)\frac{1}{m!}\frac{\partial^m\hat{f}(\eta;p)}{\partial p^m}\Big|_{p=0}. \tag{2.20}$$

2.2.2.2 mth-order deformation problem

Differentiating the zeroth-order deformation problem (2.16) and (2.17) m−times with respect to p and then dividing by $m!$ and finally setting $p=0$, we obtain the following mth-order deformation problem.

$$\mathcal{L}[f_m(\eta)-\chi_m f_{m-1}(\eta)]=\hbar R_m(\eta), \tag{2.21}$$

Boundary conditions are:

$$f_m(\eta) = 0,\ f'_m(\eta) = 0,\ at\ \eta = 0,$$

$$f'_m(\eta) = 0,\ as\ \eta \to \infty. \tag{2.22}$$

where

$$R_m(\eta) = Af'''_{m-1} - \sum_{k=0}^{m-1} f'_{m-1-k} f'_k + (1 - \chi_m)\frac{d^2}{c^2} + \psi(\eta), \tag{2.23}$$

where,

for $n = 0$

$$\psi(\eta) = 0, \tag{2.24}$$

for $n = 1$

$$\psi(\eta) = \sum_{k=0}^{m-1} f_{m-1-k} f''_k + f'''_{m-1}, \tag{2.25}$$

for $n = 2$

$$\psi(\eta) = \frac{4}{3}\sum_{k=0}^{m-1} f_{m-1-k} f''_k + 2sgn\left(\frac{d}{c} - 1\right) \times \sum_{k=0}^{m-1} f''_{m-1-k} f'''_k, \tag{2.26}$$

for $n = 3$

$$\psi(\eta) = \frac{3}{2}\sum_{k=0}^{m-1} f_{m-1-k} f''_k + 3\sum_{k=0}^{m-1} f''_{m-1-k} f'''_k \sum_{l=0}^{k} f''_{k-l} f'''_l, \tag{2.27}$$

2.3 Results and discussion

To demonstrate the behavior of the analytic solution of Eqs. (2.7) and (2.8) by the HAM, the velocity profiles are plotted for several values of the power index n, and the material parameter A. The HAM solution is compared with the exact analytic solution in a special case and found in good agreement (table 2.1). Convergence of the series solution for $f''(0)$ is checked for some selected values of parameters in table 2.2

A	$\frac{1}{2}Re_b^{\frac{1}{2}}C_f$	
	Exact solution	HAM solution
0.0	-1	-1
0.5	−1. 2247448713	−1. 2247448711
1.0	−1. 4142135623	−1. 4142135624
1.5	−1. 5811388300	−1. 5811377715
2.0	−1. 7320508075	−1. 7320508578
2.5	−1. 8708286933	−1. 8708450311
3.0	-2	−2. 0000169533

Table 2.1: Comparison of HAM and the exact solutions when $d/c = 0.2$ and $n = 1$

m	$f''(0)$	
	$n = 1$	$n = 2$
2	−0.649583	−0.710029
5	−0.649056	−0.702227
10	−0.649203	−0.704317
13	−0.649199	−0.704023
15	−0.649199	−0.704058
18	−0.649199	−0.704114
20	−0.649199	−0.704107
25	−0.649199	−0.704097
27	−0.649199	−0.704097
30	−0.649199	−0.704097

Table 2.2: Convergence of the series solution for $f''(0)$ when $A = 1$ and $d/c = 0.2$

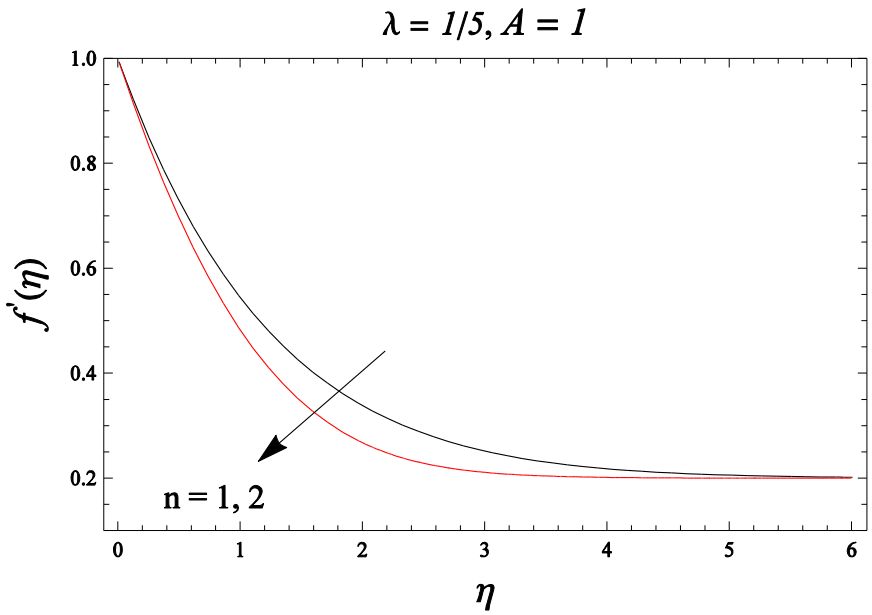

Figure 2.1: The velocity profile $f'(\eta)$ for various values of the power index n when $A = 1$.

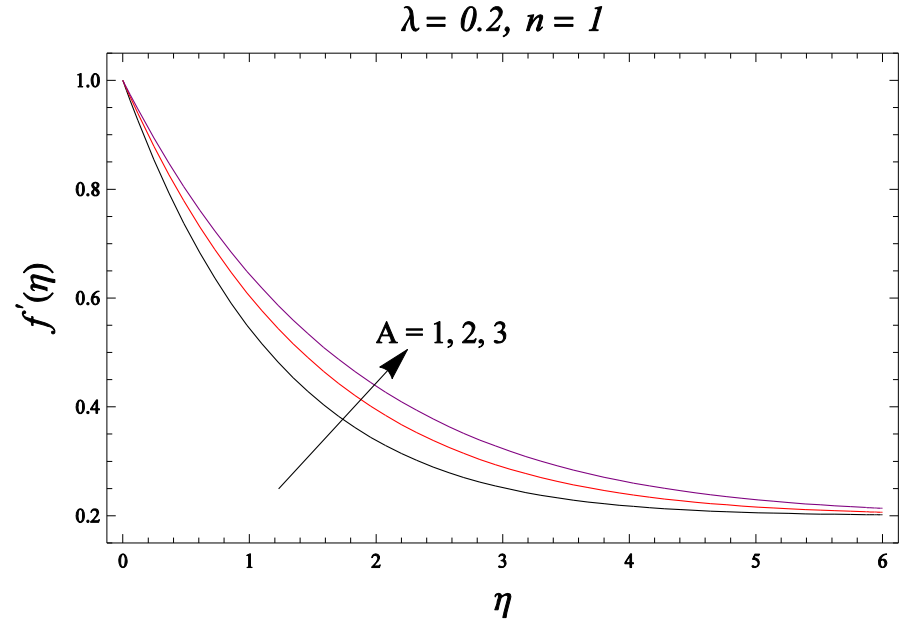

Figure 2.2: The velocity profile $f'(\eta)$ for various values of the material parameter A when $d/c = 0.2$.

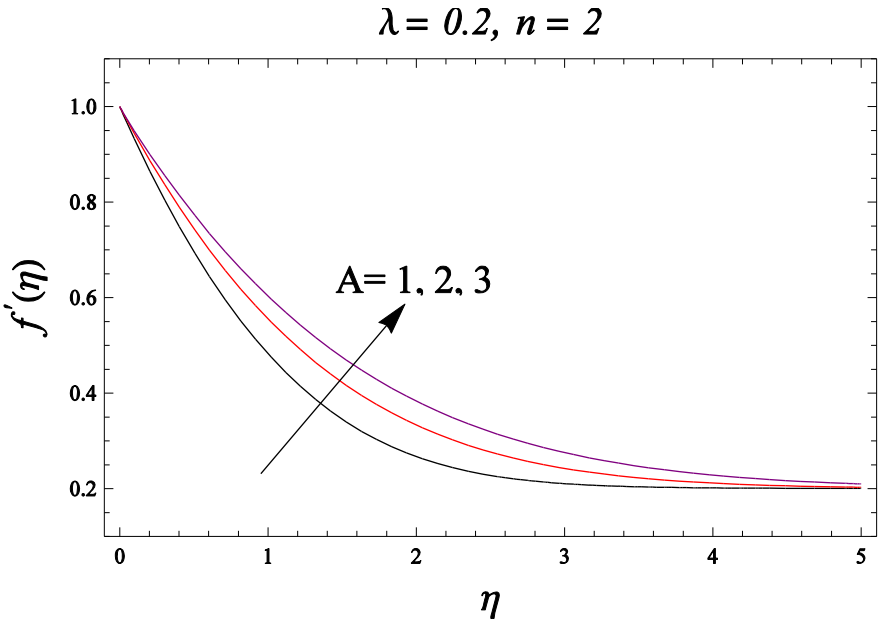

Figure 2.3: The velocity profile $f'(\eta)$ for various values of the material parameter A when $d/c = 0.2$.

BOUNDARY LAYER FLOW OF SISKO FLUID WITH CONVECTIVE BOUNDARY CONDITION

In this chapter we investigate the heat transfer characteristics in the boundary layer flow of Sisko fluid. By using the similarity approach, the modeled non-linear partial differential equation is transformed in a system of nonlinear ordinary differential equations and then the series solutions are developed. More physically acceptable connective surface boundary conditions and Newtonian heating boundary condition are imposed for the analysis of the thermal boundary layer. The solutions are physically interpreted by plotting graphs.

3.1 Mathematical Modeling

We consider the steady, two dimensional and incompressible flow of Sisko fluid driven by a linearly stretching surface coincident with $y = 0$. The fluid occupies the region $y \geq 0$. Let $U = cx$ be the velocity of the stretching sheet where $c > 0$ is constant and we have $\partial u/\partial y < 0$.

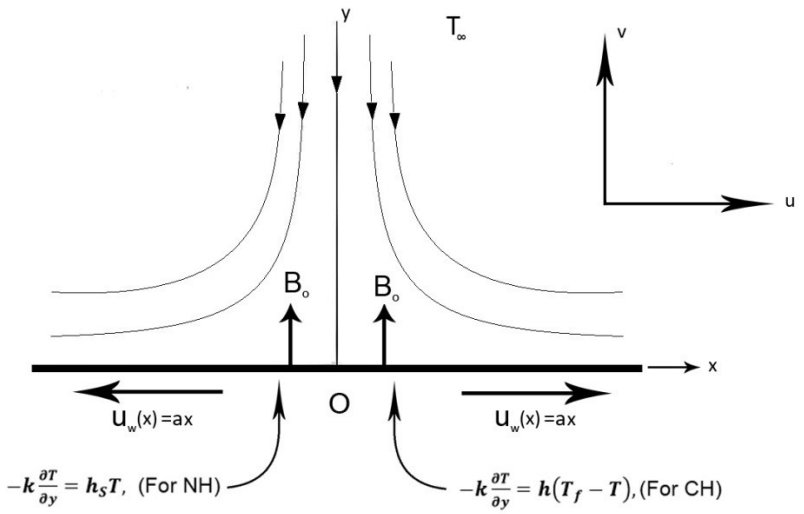

Figure 3.1: A sketch of the physical model

Boundary layer equations governing the two-dimensional flow and heat transfer of Sisko fluid can be expressed as:

$$\frac{\partial u}{\partial x}+\frac{\partial v}{\partial y}=0, \tag{3.1}$$

$$\rho\left(u\frac{\partial u}{\partial x}+v\frac{\partial u}{\partial y}\right)=a\frac{\partial^2 u}{\partial y^2}-b\frac{\partial}{\partial y}\left(-\frac{\partial u}{\partial y}\right)^n-\frac{6}{\rho}B_0^2u, \tag{3.2}$$

$$u\frac{\partial T}{\partial x}+v\frac{\partial T}{\partial y}=\alpha\frac{\partial^2 T}{\partial y^2}, \tag{3.3}$$

where u and v are the velocity components along the x and y directions respectively, T is the temperature field, a and b are the material fluid parameters, ρ is the density of the fluid and α is the thermal diffusivity.

From the above Eq (3.2), if $a=0$ the equation corresponds to the case of power law fluid and if $b=0$, Eq (3.2) reduces to the case of Newtonian fluid. The boundary conditions are:

$$\left.\begin{aligned} &u=cx,\ v=0,\ -k\frac{\partial T}{\partial y}=h\left(T_f-T\right),\ \text{(for CH)},\\ &-k\frac{\partial T}{\partial y}=h_S T,\ \text{(for NH)}\end{aligned}\right\}\ at\ y=0,$$
$$u\to 0,\ T\to T_\infty \qquad as \qquad y\to\infty. \tag{3.4}$$

In the current problem, the flow is solely created by the motion of stretching sheet. No pressure gradient contributes to the flow. We now introduce the following similarity transformations.

$$u=cxf'(\eta),\qquad v=-\left(\frac{2n}{n+1}\right)\left(\frac{b/\rho}{c^{1-2n}}\right)^{\frac{1}{n+1}}x^{\frac{n-1}{n+1}}f(\eta),$$
$$\eta=y\left(\frac{c^{2-n}}{b/\rho}\right)^{\frac{1}{n+1}}x^{\frac{1-n}{1+n}},\quad \Psi(x,y)=\left(\frac{b/\rho}{c^{1-2n}}\right)^{\frac{1}{n+1}}x^{\frac{2n}{n+1}}f(\eta),\quad \theta(\eta)=\frac{T-T_\infty}{T_f-T_\infty}, \tag{3.5}$$

Eqs (3.2) to (3.4) in view of (3.5) become:

$$Af''' + n(-f'')^{n-1}f''' + \left(\frac{2n}{n+1}\right)ff'' - f'^2 - M^2f' = 0, \tag{3.6}$$

$$\theta'' + \left(\frac{Pr}{A}\right)\left(\frac{2n}{n+1}\right)f\theta' = 0, \tag{3.7}$$

The boundary conditions are:

$$\begin{gathered} f(0) = 0, \quad f'(0) = 1, \quad f'(\infty) = 0\ , \\ \theta'(0) = -\gamma[1 - \theta(0)],\ (\text{ for CH }), \quad \theta'(0) = -\gamma[1 + \theta(0)]\ (\text{ for NH }) \\ \theta(\infty) = 0. \end{gathered} \tag{3.8}$$

where γ and Pr is the Biot number and Prandlt number respectively. These defined as under:

$$\gamma = \frac{h_f}{k}\left(\frac{c^{2-n}}{b/\rho}\right)^{\frac{-1}{n+1}} x^{\frac{n-1}{n+1}}, \quad Pr = \frac{\upsilon}{\alpha}.$$

The quantity of physical interest is the skin friction coefficient C_f which is defined as:

$$C_f = \tau_w/\left(\frac{1}{2}\rho U^2\right), \tag{3.9}$$

where $\tau_w = \left(a + b\left|\frac{\partial u}{\partial y}\right|^{n-1}\right)\frac{\partial u}{\partial y}\Big|_{y=0}$ is wall shear stress. Using variables from Eq (3.5), Eq (3.10) reduces to:

$$\frac{1}{2}C_f Re_b^{\frac{1}{n+1}} = Af''(0) — [-f''(0)]^n, \tag{3.10}$$

The local Nusselt number Nu_x may be found in terms of the dimensionless temperature at the wall surface, $\theta'(0)$, that is

$$Re_b^{\frac{1}{n+1}} Nu_x = -\theta'(0), \tag{3.11}$$

with $Nu_x = \frac{xq_w}{k(T_f - T_\infty)}$ with q_w as the surface heat flux.

3.2 Analytic Solution

We use HAM in order to solve the set of equations (3.6) and (3.7) with the conditions (3.8).

Firstly we choose the initial guess and auxiliary linear operator i.e.

$$f_0(\eta) = 1 - e^{-\eta} \quad , \quad \theta_0(\eta) = \frac{\gamma e^{-\eta}}{1+\gamma} \text{ (CH)}, \qquad \theta_0(\eta) = \frac{\gamma e^{-\eta}}{1-\gamma} \text{ (NH)}, \tag{3.12}$$

$$L_f = \frac{\partial^3 f}{\partial \eta^3} - \frac{\partial f}{\partial \eta} \quad , \quad L_\theta = \frac{\partial^2 \theta}{\partial \eta^2} - \theta. \tag{3.13}$$

The operator L_f and L_θ satisfy,

$$L_f[C_1 + C_2 \exp(-\eta) + C_3 \exp(\eta)] = 0,$$

$$L_f[C_4 + C_5 \exp(-\eta)] = 0,$$

where C_1, C_2, C_3, C_4 and C_5 are the arbitrary constants.

3.2.1 Zero-order deformation problem

Now the problem related to zero-order deformation is

$$f(1-p)L_f\left[\hat{f}(\eta;p) - f_0(\eta)\right] = p\hbar N_f\left[\hat{f}(\eta;p)\right].$$
$$(1-p)L_\theta\left[\hat{\theta}(\eta;p) - \theta_0(\eta)\right] = p\hbar N_\theta\left[\hat{\theta}(\eta;p)\right], \tag{3.14}$$

$$\left.\begin{aligned} \hat{f}(\eta;p) = 0,\ \hat{f}'(\eta;p) = 1, \\ \hat{\theta}'(\eta;p) = -\gamma\left[1 - \hat{\theta}(\eta;p)\right], \quad \text{(for CH)} \\ \hat{\theta}'(\eta;p) = -\gamma\left[1 + \hat{\theta}(\eta;p)\right], \quad \text{(for NH)} \end{aligned}\right\} \ at\ \eta = 0, \tag{3.15}$$

$$\hat{f}'(\eta;p) = 0,\ \hat{\theta}(\eta;p) = 0 \ \text{ as } \eta \to \infty. \tag{3.16}$$

where nonlinear differential operator N_f and N_θ are:

$$N_f\left[\hat{f}(\eta;p)\right] = A\frac{\partial^3 \hat{f}(\eta;p)}{\partial \eta^3} + n\left[-\frac{\partial^2 \hat{f}(\eta;p)}{\partial \eta^2}\right]^{n-1}\frac{\partial^3 \hat{f}(\eta;p)}{\partial \eta^3} \tag{3.17}$$

$$+\left(\frac{2n}{n+1}\right)\hat{f}(\eta;p)\frac{\partial^2 \hat{f}(\eta;p)}{\partial \eta^2} - \frac{\partial \hat{f}(\eta;p)}{\partial \eta}\frac{\partial \hat{f}(\eta;p)}{\partial \eta} - M^2\frac{\partial \hat{f}(\eta;p)}{\partial \eta},$$

$$N_\theta\left[\hat{\theta}(\eta;p)\right] = \frac{\partial^2\hat{\theta}(\eta;p)}{\partial\eta^2} + \left(\frac{Pr}{A}\right)\left(\frac{2n}{n+1}\right)\hat{f}(\eta;p)\frac{\partial\hat{\theta}(\eta;p)}{\partial\eta}, \tag{3.18}$$

where $p \in [0,1]$ is a homotopy parameter and $\hbar \neq 0$ is an auxiliary parameter. At $p = 0$ and $p = 1$ we have, respectively:

$$\begin{aligned} \hat{f}(\eta;0) = f_0(\eta),\ \hat{f}(\eta;1) = f(\eta), \\ \hat{\theta}(\eta;0) = \theta_0(\eta), \quad \hat{\theta}(\eta;1) = \theta(\eta). \end{aligned} \tag{3.19}$$

When the parameter p varies from zero to unity the solution $\hat{f}(\eta;p)$ through the initial guess $f_0(\eta)$ approaches $f(\eta)$ respectively. Now we expand the function $\hat{f}(\eta;p)$ by using Taylor's series about $p = 0$ and then substituting $p = 1$, we get:

$$\begin{aligned} f(\eta) = f_0(\eta) + \textstyle\sum_{m=1}^{\infty} f_m(\eta), \ \text{ where } \quad f_m(\eta)\frac{1}{m!}\frac{\partial^m\hat{f}(\eta;p)}{\partial p^m}\Big|_{p=0}, \\ \theta(\eta) = \theta_0(\eta) + \textstyle\sum_{m=1}^{\infty} \theta_m(\eta), \ \text{ where } \quad \theta_m(\eta)\frac{1}{m!}\frac{\partial^m\hat{\theta}(\eta;p)}{\partial p^m}\Big|_{p=0}. \end{aligned} \tag{3.20}$$

3.2.2 mth-order deformation problem

Differentiating the zeroth-order deformation problem (3.14) and (3.16) m−times with respect to p and then dividing by $m!$ and finally setting $p = 0$, we obtain the following mth-order deformation problem.

$$L_f[f_m(\eta) - \chi_m f_{m-1}(\eta)] = \hbar R^f{}_m(\eta), \tag{3.21}$$

$$L_\theta[\theta_m(\eta) - \chi_m \theta_{m-1}(\eta)] = \hbar R^\theta{}_m(\eta), \tag{3.22}$$

Boundary conditions are:

$$\left.\begin{aligned} f_m(\eta) = 0,\ f'_m(\eta) = 0,\ \theta'_m(\eta) - \gamma[\theta_m(\eta)] = 0, \ \text{ (for CH)} \\ \theta'_m(\eta) + \gamma[\theta_m(\eta)] = 0, \ \text{ (for NH)} \end{aligned}\right\} \ at\ \eta = 0, \qquad f'_m(\eta) = 0,\ \theta_m(\eta) = 0\ as\ \eta \to \infty, \tag{3.23}$$

where

$$R^f{}_m(\eta) = Af'''_{m-1} - \textstyle\sum_{k=0}^{m-1} f'_{m-1-k} f'_k + \psi(\eta), \tag{3.24}$$

$$R^{\theta}{}_{m}(\eta) = \theta''{}_{m-1} + \frac{Pr}{A}\left(\frac{2n}{n+1}\right)\sum_{k=0}^{m-1}\theta'{}_{m-1-k}f_{k}, \tag{3.25}$$

$$\chi_m = \begin{cases} 0 & m \leq 1 \\ 1 & m > 1 \end{cases}$$

The linear non-homogeneous problems (3.21) − (3.23) can be solved by using any symbolic computational software like MATHEMATICA in the order m = 1, 2, 3….

3.3 Results and Discussions

This section shows the effects of various parameters on both the velocity and temperature profiles. The velocity and temperature distributions are given for several values of the embedded parameters, namely, the power index n, the material parameter A, magnetic field M, biot number γ, and the Prandtl number Pr. The analytic solution contains the convergence control parameter $\hbar$, which can ensure the convergence of the solutions. Figure 3.2 gives the convergence region for $f''(0)$ at a given order of approximation.

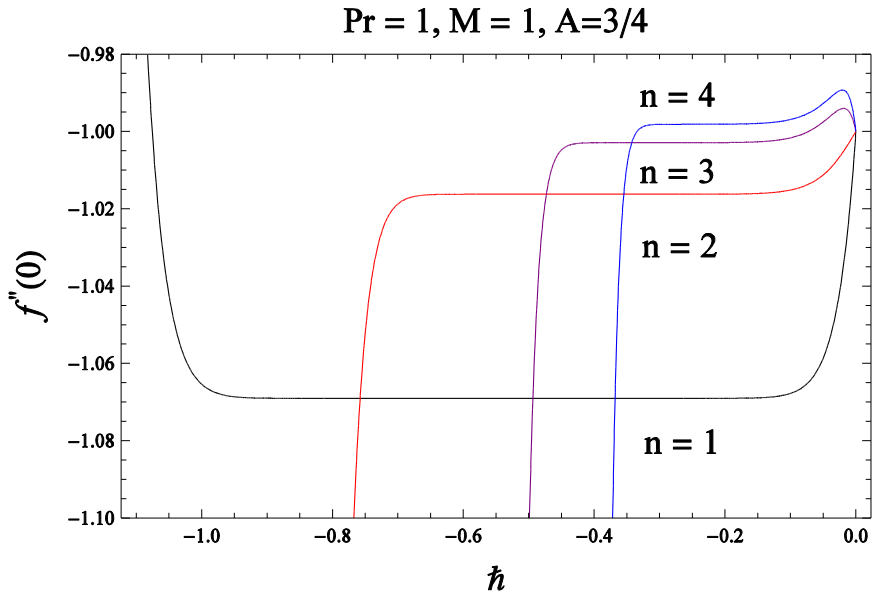

Figure 3.2: The *h* curves of $f''(0)$ for A = 3/4 at 20th order of approximation.

Here the valid region for $\hbar$ curves are -0.9 < $\hbar$ < -0.2, -0.7 < $\hbar$< -0.2, -0.4 < $\hbar$ < -0.2, -0.3 < $\hbar$ < -0.25 for n=1, 2, 3 and 4 respectively. Figure 3.3 shows the convergence region and rate of approximation of $f''(0)$ for the obtained analytic solution for different values of A for n=2.

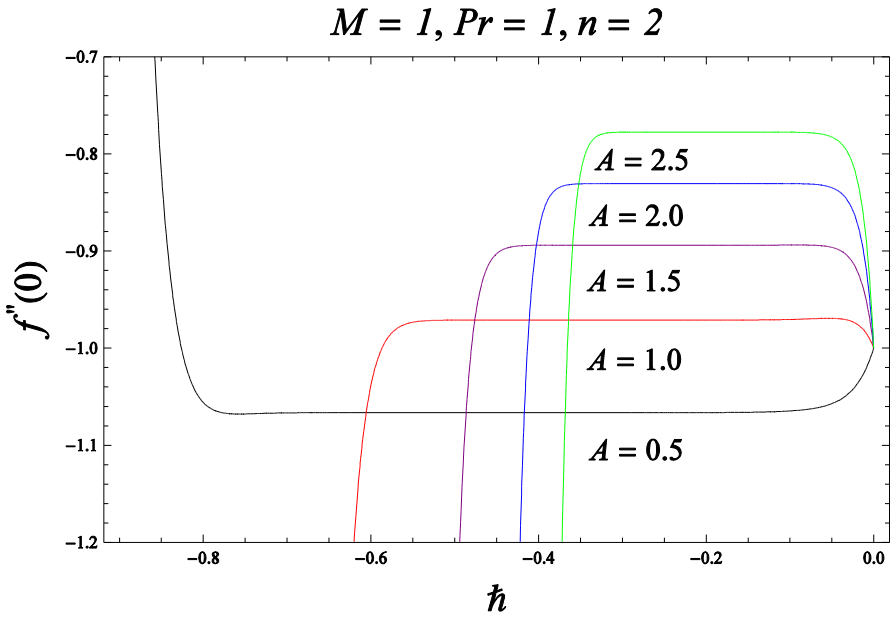

Figure 3.3: The $\hbar$ curves of $f''(0)$ for $n = 2$ at 20th order of approximation.

Here the valid region for $\hbar$ curves is -0.8 < $\hbar$ < -0.1, -0.58 < $\hbar$ < -0.1, -0.45 < $\hbar$ < -0.1, -0.4 < $\hbar$ < -0.1 and -0.38 < $\hbar$ < -0.1 for A = 0.5, 1, 1.5, 2, 2.5 respectively.

Figure 3.4 shows the convergence region and rate of approximation of $\theta'(0)$ for the obtained analytic solution for different values of power index n for convective heating.

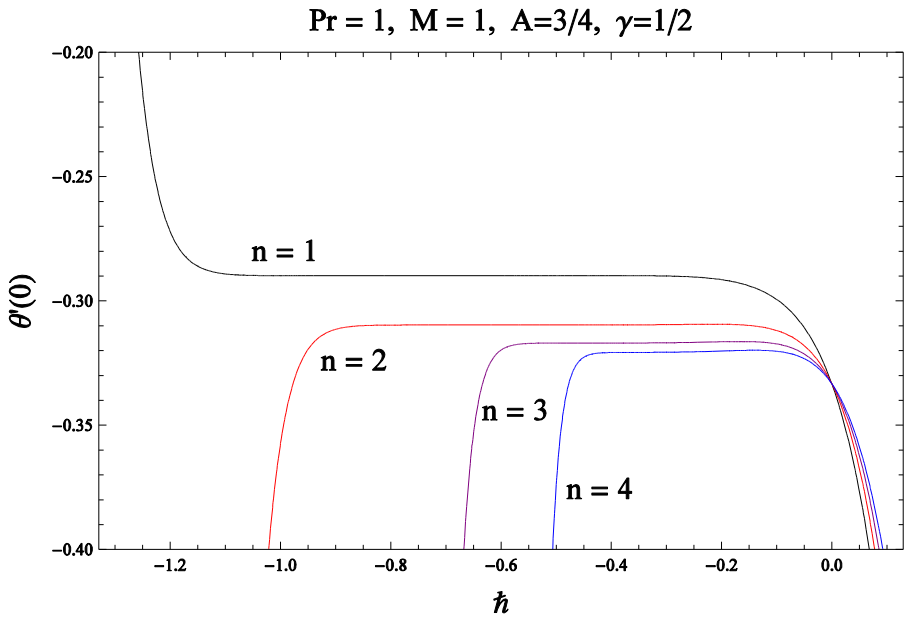

Figure 3.4: The $\hbar$ curves of $\theta'(0)$ at 20th order approximation in case of Convective heating boundary condition.

Here the valid region for $\hbar$ curves is -1.25 < $\hbar$ < -0.2, -0.9 < $\hbar$ < -0.1, -0.6 < $\hbar$ < -0.1 and -0.48 < $\hbar$ < -0.1 for n = 1, 2, 3 and 4 respectively.

Figure 3.5 shows the convergence region and rate of approximation of $\theta'(0)$ for the obtained analytic solution for different values of power index n for Newtonian heating.

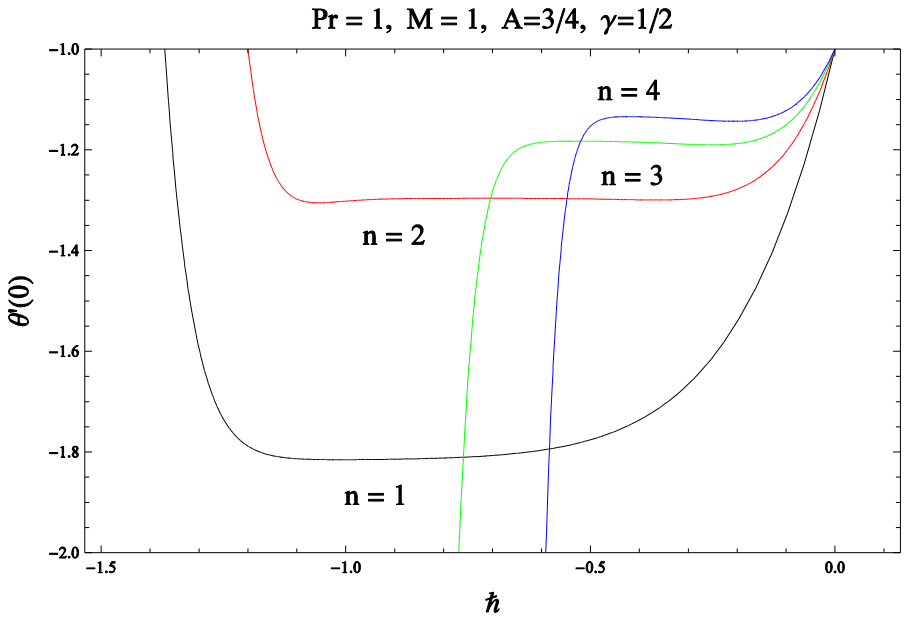

Figure 3.5: The $\hbar$ curves of $\theta'(0)$ at the 15th order approximation in case of Newtonian heating boundary condition.

Here the valid region for $\hbar$ curves is -1.2 < $\hbar$ < -0.5, -1.1 < $\hbar$ < -0.3, -0.7 < $\hbar$ < -0.2 and -0.5 < $\hbar$ < -0.1 for n = 1, 2, 3 and 4 respectively.

Figure 3.6 shows the convergence region and rate of approximation of $\theta'(0)$ for the obtained analytic solution for different values of A.

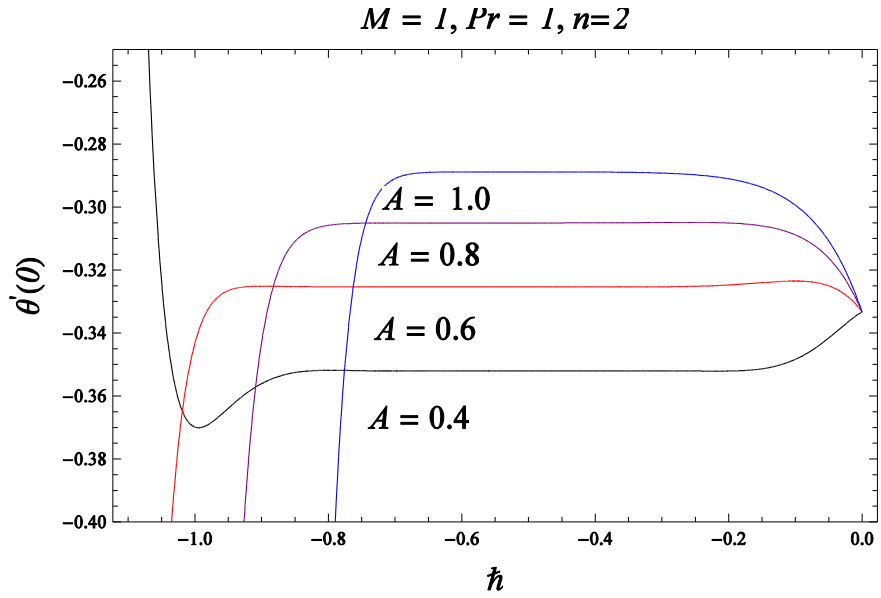

Figure 3.6: The $\hbar$ curves of $\theta'(0)$ for $n = 2$ at 20th order approximation.

Here the valid region for $\hbar$ curves is -0.85 < $\hbar$ < -0.2, -1.0 < $\hbar$ < -0.15, -0.83 < $\hbar$ < -0.15 and -0.79 < $\hbar$ < -0.18 for $A = 0.4, 0.6, 0.8$ and 1 respectively.

The effects of the material parameter of the Sisko fluid A on velocity profile f' are shown in Figure 3.7. This figure shows that the fluid velocity f' increases when there is an increase in A. Similarly the effects of the magnetic field M are shown in Figure 3.8. This figure shows that the fluid velocity f' decreases when there is an increase in M.

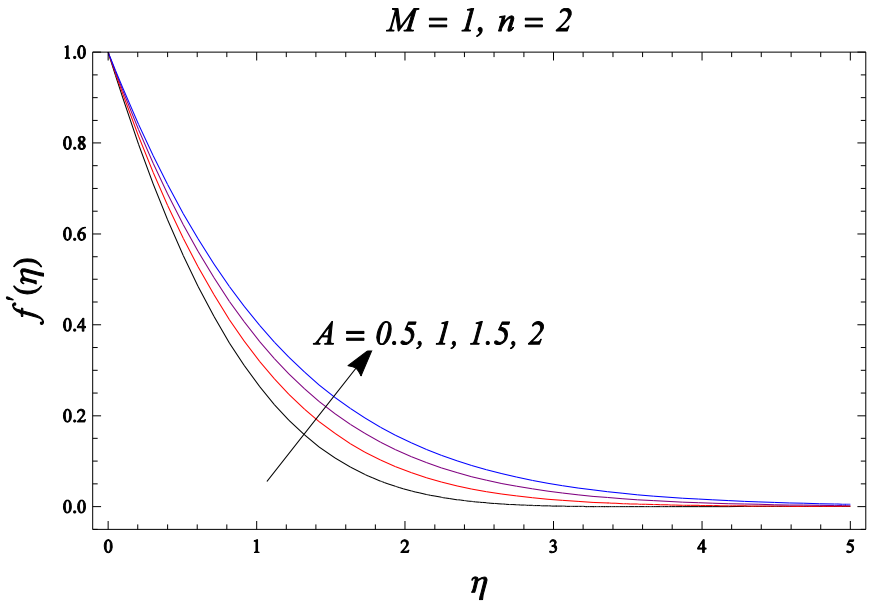

Figure 3.7: The velocity profiles $f'(\eta)$ for various values of *A*.

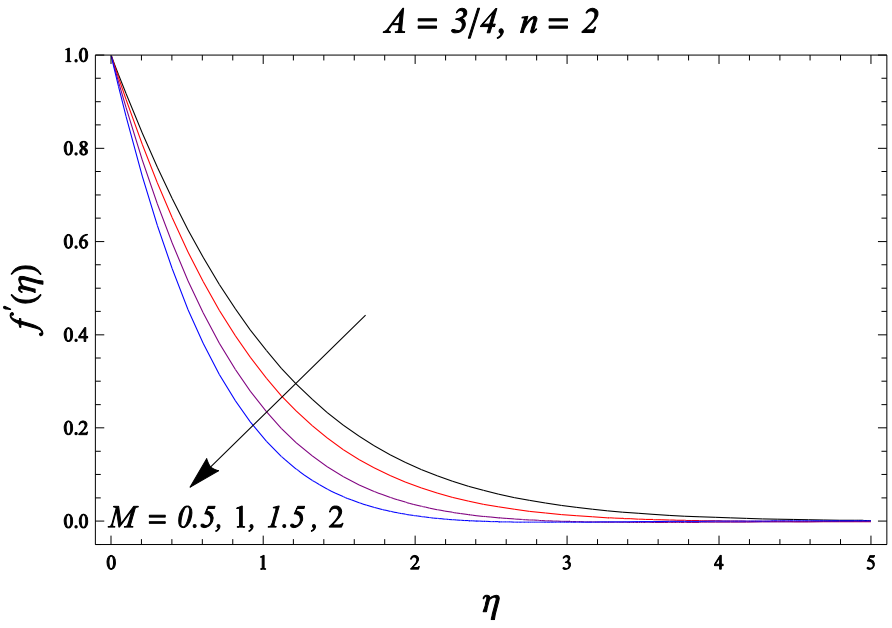

Figure 3.8: The velocity profiles $f'(\eta)$ for various values of *M*.

Figure 3.9 shows the variation of Prandtl number Pr on θ for convective heating. The temperature profile θ decreases when Pr increases. Similarly figure 3.10 shows the variation of Prandtl number Pr on θ for Newtonian heating. The temperature profile θ decreases when Pr increases.

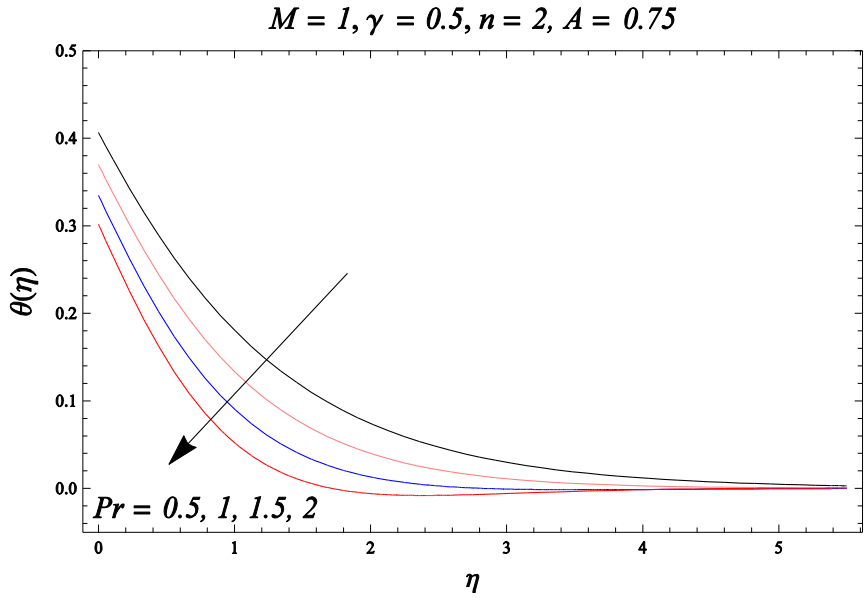

Figure 3.9: The temperature function $\theta(\eta)$ for various values of Pr in case of convective heating boundary condition.

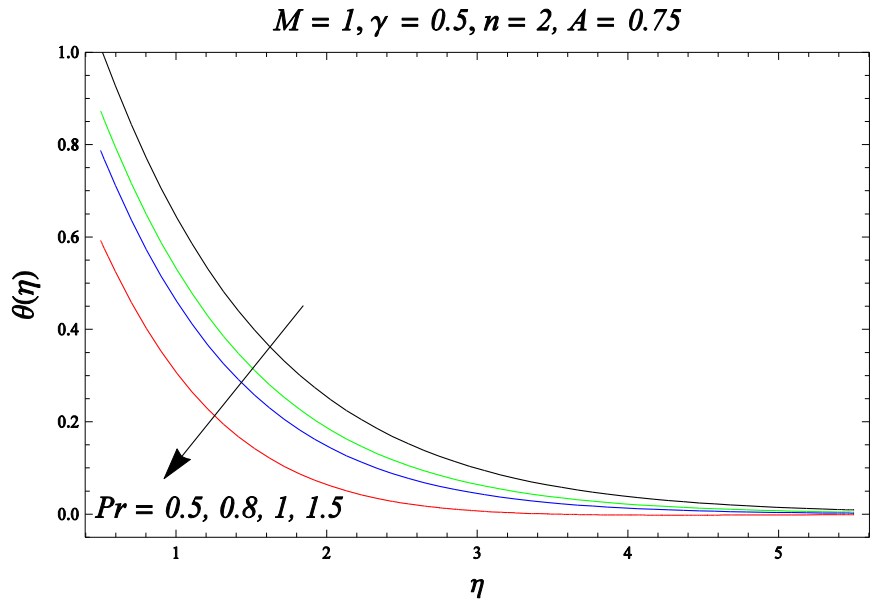

Figure 3.10: The temperature function $\theta(\eta)$ for various values of Pr in case of Newtonian heating boundary condition.

Figure 3.11 shows the effect of A on θ for convective heating, The temperature profile increases by increasing the values of A. Figure 3.12 shows the effect of A on θ for Newtonian heating, The temperature profile increases by increasing the values of A.

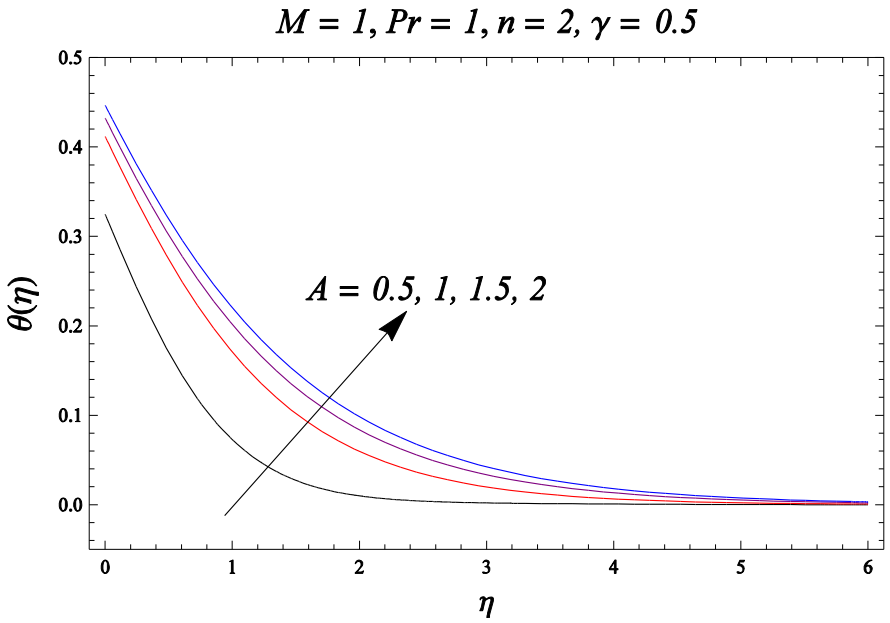

Figure 3.11: The temperature function $\theta(\eta)$ for various values of A in case of convective heating boundary condition.

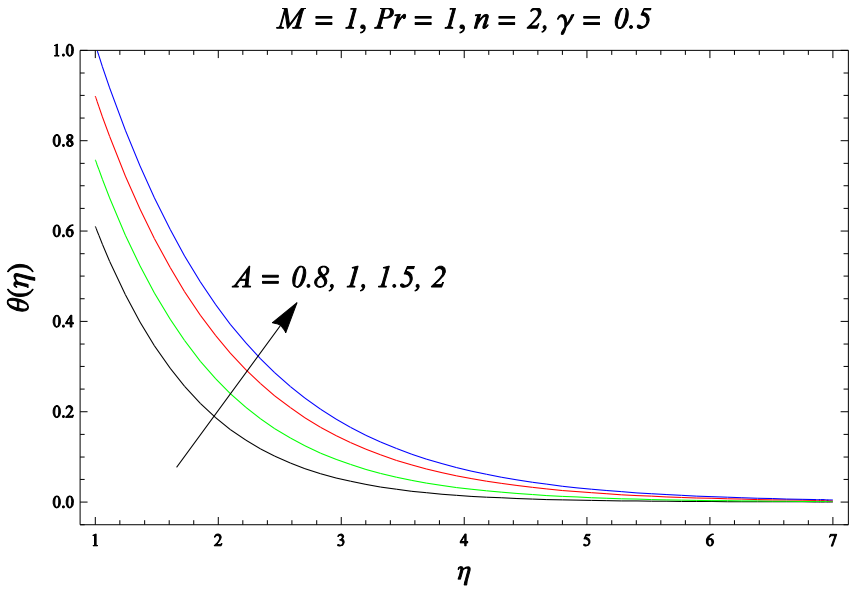

Figure 3.12: The temperature function $\theta(\eta)$ for various values of A in case of Newtonian heating boundary condition.

Figure 3.13 shows the effect of Biot number γ on θ for convective heating. We can see that when $\gamma = 0$ then there is no heat transfer and there is no temperature change. The temperature profile θ increases when γ increases. Similarly figure 3.14 shows the effect of Biot number γ on θ for Newtonian heating. We can see that when $\gamma = 0$ then there is no heat transfer and there is no temperature change. The temperature profile θ increases when γ increases.

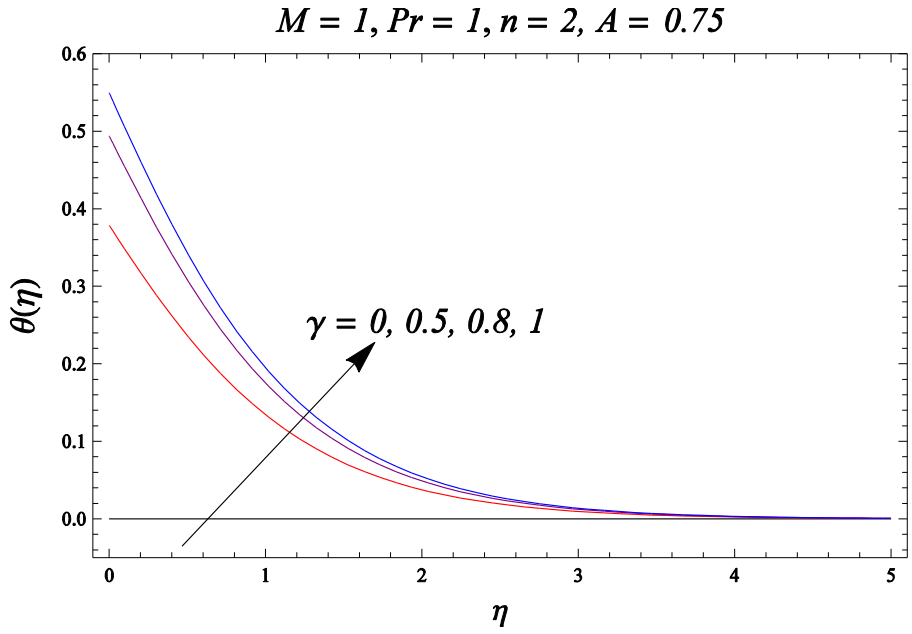

Figure 3.13: The temperature function $\theta(\eta)$ for various values of γ in case of convective heating boundary condition.

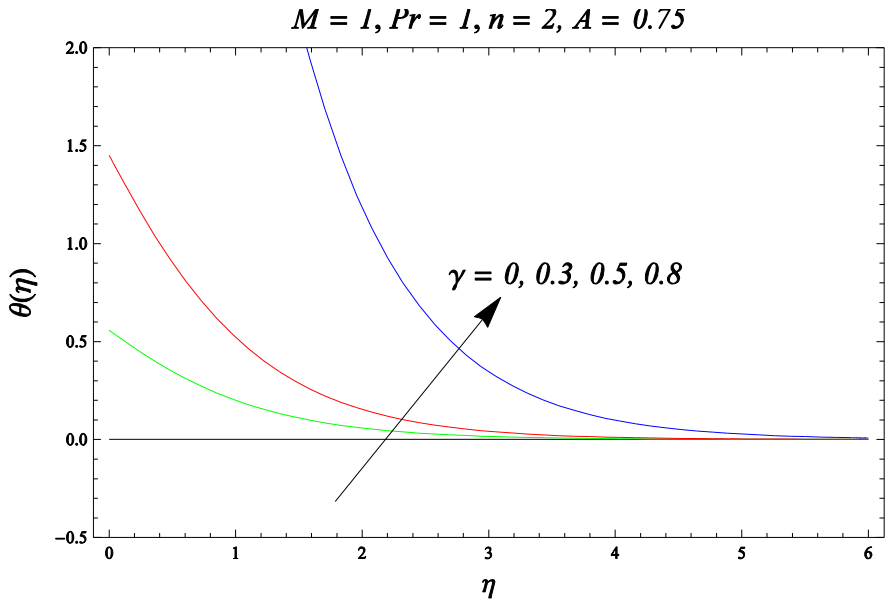

Figure 3.14: The temperature function $\theta(\eta)$ for various values of γ in case of Newtonian heating boundary condition.

Figure 3.15 shows the effect of M on θ for convective heating. The temperature profile θ increases when M increases. Similarly figure 3.16 shows the effect of M on θ for Newtonian heating. The temperature profile θ increases when M increases.

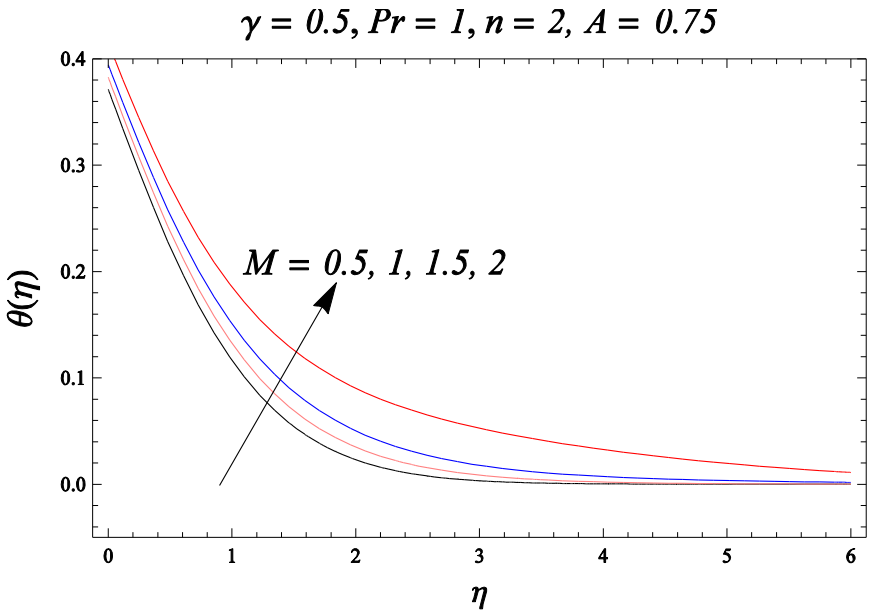

Figure 3.15: The temperature function $\theta(\eta)$ for various values of M in case of convective heating boundary condition.

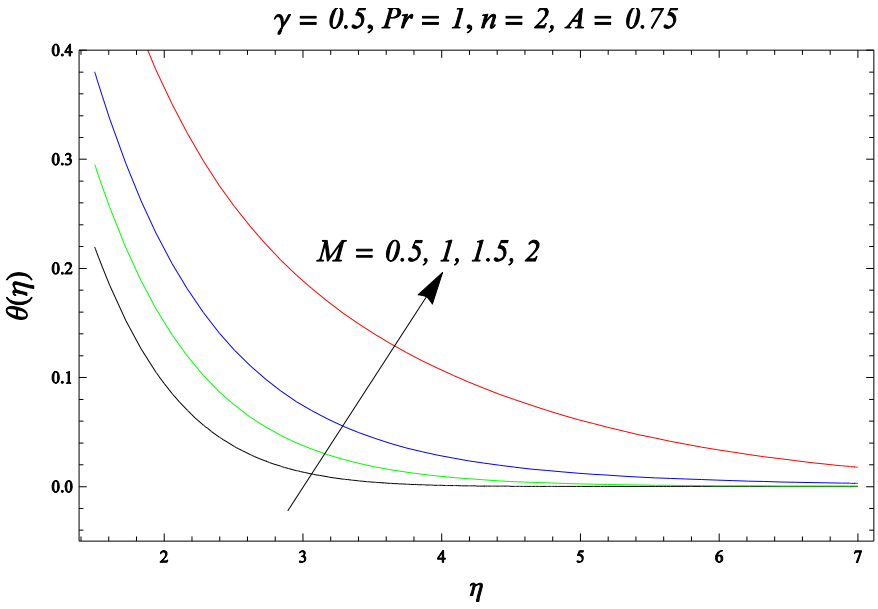

Figure 3.16: The temperature function $\theta(\eta)$ for various values of M in case of Newtonian heating boundary condition.

Figure 3.17 shows the variation of local Nusselt number with the change in Biot number γ. It is clearly observed from the plots that the heat transfer rate increases with the increase in the Prandtl number Pr. Figure 3.18 shows the variation of local Nusselt number with the change in fluid material parameter A. It is clearly observed from the plots that the heat transfer rate decreases with the increase in the magnetic field M.

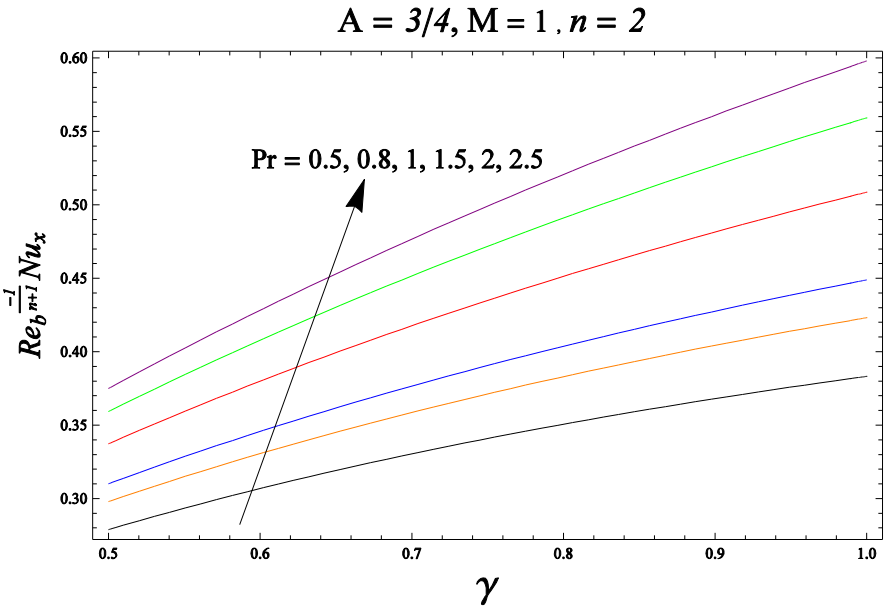

Figure 3.17: The variation of the local Nusselt number with γ for different values of Pr

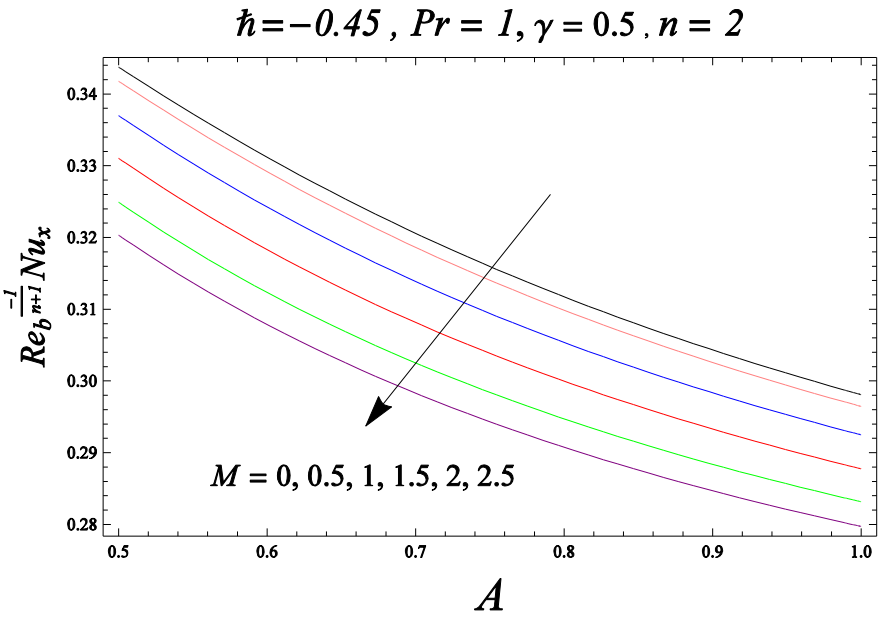

Figure 3.18: The variation of the local Nusselt number with A for different values of M

Figure 3.19 shows the variation of local skin friction coefficient with the change in fluid material parameter$A$.

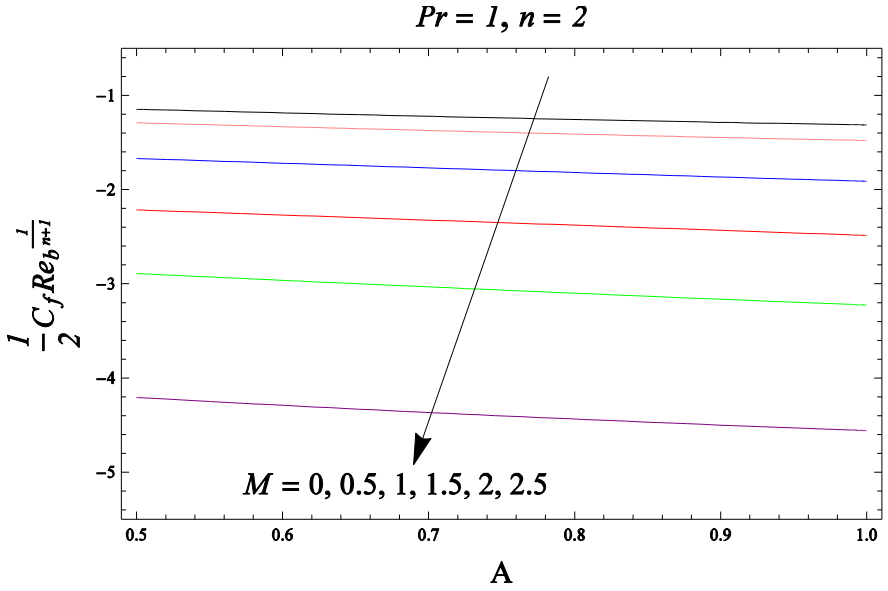

Figure 3.19: The variation of the local skin friction coefficient with A for different values of M

Convergence of the series solution for $f''(0)$ and $\theta'(0)$ when $A = 1$ is shown in Table 3.1.

m	$n = 2$	
	$f''(0)$	$\theta'(0)$
2	-0.975	-0.309919
5	-0.970533	-0.295703
10	-0.971258	-0.289878
15	-0.97122	-0.289015
20	-0.971223	-0.288906
25	-0.971222	-0.288897
27	-0.971222	-0.288897
29	-0.971222	-0.288897
30	-0.971222	-0.288897

Table 3.1: Convergence of the series solution of $f''(0)$ and $\theta'(0)$ when $A = 1$.

References

1. H. Blasius. The Boundary Layer in Fluids with Little Friction, NASA, technical memorandum, 1256, Washington 1950, translation of grenzschichten in flussigkeiten mit kleiner reibung. Technical Report 56 1908.
2. B.C. Sakiadis, Boundary-layer Behaviour on Continuous Solid Surfaces, AIChE J. 7 (1961) 26–28.
3. L. J. Crane, Flow Past a Stretching Sheet, Z. Angew. Math. Phys. 21 (1970) 645–647.
4. C. K. Chen and M. I. Char, Heat transfer on a continuous stretching surface with suction or blowing, J. Math. Anal. Appl. 135 (1988) 568-580.
5. R. Cortel, Viscous Flow and Heat Transfer over a Nonlinearly Stretching Sheet Appl. Math. Comput. 184 (2007) 864–873.
6. W. R. Schowalter, The Application of Boundary Layer Theory to Power Law Pseudoplastic Fluids: Similar Solutions, AIChE J. 6 (1960) 24-28.
7. K. R. Rajagopal, T. Y. Na, and A. S. Gupta Flow of a Viscoelastic Fluid over a Stretching Sheet, Rheol Acta 23 (1984) 213-215.
8. S. Y. Lee and W. F. Ames, Similar Solutions for Non-Newtonian Fluids, AIChE J. 12 (1966) 700–708.
9. K. Vajravelu and D. Rollins, Heat Transfer in a Viscoelastic Fluid over a Stretching Sheet, J. Math. Anal. Appl. 158 (1991) 241-255.
10. H. I. Andersson, K. H. Bech and B. S. Dandapat, Magnetohydrodynamic Flow of a Power-law Fluid over a Stretching Sheet, Int. J. Non-Linear Mech. 27 (1992) 929–936.
11. K. Vajravelu, T. Roper, Flow and Heat Transfer in a Second Grade over a Stretching Sheet, Int. J. Non-Linear Mech. 34 (1999) 1031-1036.

12. H. Xu , S. J. Liao, Laminar Flow and Heat Transfer in the Boundary-Layer of Non-Newtonian Fluids over a Stretching Flat Sheet, Comp. Math. Appl. 57 (2009) 1425-1431.
13. A. W. Sisko, The Flow of Lubricating Greases, Ind. Eng. Chem. Res 50 (1958) 1789–1792.
14. M. Khan, Z. Abbas, T. Hayat, Analytic Solution for Flow of Sisko Fluid through a Porous Medium, Transp. Porous Med. 71 (2008) 23–37.
15. T. Hayat, R. J. Moitsheki and S. Abelman, Stokes' First Problem for Sisko Fluid over a Porous Wall, App. Math. Comput. 217 (2010) 622-628.
16. M. Khan, A. Shahzad, On Stagnation Point Flow of Sisko Fluid over a Stretching Sheet, Meccan. 48 (2013) 2391-2400.
17. A. Aziz, A Similarity Solution for Laminar Thermal Boundary Layer over a Flat Plate with a Convective Surface Boundary Condition, Commun. Nonlinear Sci. Numer. Simul. 14 (2009) 1064-1068.
18. S. Yao, T. Fang and Y. Zhong, Heat Transfer of a Generalized Stretching/Shrinking Wall Problem with Convective Boundary Conditions, Commun. Nonlinear Sci. Numer. Simul. 16 (2011) 752-760.
19. A. Ishak, Similarity Solutions for Flow and Heat Transfer over a Permeable Surface with Convective Boundary Condition, Comp. Math. Appl. 217 (2010) 837-842.
20. O. D. Makinde, A. Aziz, Boundary Layer Flow of a Nanofluid Past a Stretching Sheet with a Convective Boundary Condition, Int. J. Ther. Sci. 50 (2011) 1326-1332.
21. O. D. Makinde, A. Aziz, MHD Mixed Convection from a Vertical Plate Embedded in a Porous Medium with a Convective Boundary Condition, Int. J. Ther. Sci. 49 (2010) 1813-1820.

22. T. Hayat, S. A. Shehzad, M. Qasim, and S. Obaidat Flow of a Second Grade Fluid with Convective Boundary Conditions, Therm. Sci. 15 (2011) 253-261.
23. S. J. Liao, Homotopy Analysis Method: A New Analytic Method for Nonlinear Problems. Appl. Math. Mech. 19, No. 10, Oct. (1998)
24. S.J. Liao Notes on the Homotopy Analysis Method: Some Definitions and Theorems Comm. in Non-linear Sci. & Numerical Simulation 14 (2009) 983–997.
25. Liao, S.J Beyond Perturbation – Introduction to the Homotopy Analysis Method Chapman & Hall/ CRC Press, Boca Raton (2003).
26. S.J. Liao On the Homotopy Analysis Method for Nonlinear Problems Appl. Math. Comput. 147 (2004) 499-513.
27. S.J. Liao, A Uniformly Valid Analytic Solution of 2D Viscous Flow Past a Semi-Infinite Flat Plate, J. Fluid Mech. 385 (1999) 101-128.
28. S.J. Liao and A. Campo, Analytic Solutions of the Temperature Distribution Blasius Viscous Flow Problems, J. Fluid Mech. 453 (2002) 411-425.
29. M. Ayub, A. Rasheed and T. Hayat, Exact Flow of a Third Grade Fluid Past a Porous Plate using Homotopy Analysis Method, Int. J.Engg. Sci. 41 (2003) 2091-2103.
30. T. Hayat, M. Khan and M. Ayub, On the Explicit Analytic Solutions of an Oldroyd 6-Constant Fluid, Int. J.Engg. Sci. 42 (2004) 123-135.
31. T. Hayat, M. Khan and M. Ayub, Couette and Poiseuille Flows of an Oldroyd 6-Constant Fluid with Magnetic Field, J. Math. Anal. & Appl. 298 (2004) 225-244.
32. A.M. Lyapunov, General Problem on Stability of Motion, Taylor & Francis, London, 1992 (English translation).
33. A.V. Karmishin, A.I. Zhukov, V.G. Kolosov, Methods of Dynamics Calculation and Testing for Thin-Walled Structures, Mashinostroyenie, Moscow 1990.

34. G. Adomian, Solving Frontier Problems of Physics: The Decomposition Method, Kluwer Academic, Dordrecht 1994.